International Applied Mechanics, Vol. 47, No. 4, October, 2011 (Russian Original Vol. 47, No. 4, July, 2011)

STRESS CONCENTRATION IN A TRANSVERSELY ISOTROPIC SPHERICAL SHELL WITH TWO CIRCULAR RIGID INCLUSIONS

V. N. Chekhov[1] and S. V. Zakora[2]

The refined Timoshenko-type theory that takes into account the transverse shear strains is used to find an analytic solution for the stress state of transversely isotropic shallow spherical shell with two circular rigid inclusions. The case of a shell with closely spaced rigid inclusions of unequal radii under internal pressure is analyzed numerically. The stresses in the shell increase considerably with decrease in the distance between the inclusions and increase in the transverse shear parameter

Keywords: stress concentration, transversely isotropic shallow spherical shell, circular rigid inclusion, transverse shear

Introduction. Despite their long history [1–3], studies of stress concentration in plates and shells with holes and inclusions (rings, washers, covers) are still relevant [5–8]. A similar situation exists with other problems in the mechanics for multiply connected and structurally inhomogeneous bodies [4, 9]. Analytic solutions and numerical results of stress analysis of shallow spherical shells with two or more holes reinforced with highly rigid rings are available only for the case of an isotropic shell with identical circular holes [1–3]. The minimum width of the bridge between the reinforced holes in this case is 0.7 of the hole radius. However, if the holes are closely spaced, the stress concentration is much higher, as is the case in a plate with two holes under tension [8]. Therefore, we will consider a transversely isotropic shallow spherical shell with two closely spaced circular perfectly rigid inclusions of different radii.

1. Problem Formulation. Consider a transversely isotropic shallow spherical shell with two circular rigid inclusions of different radii (Fig. 1). The shell is subjected to uniform internal pressure $p = \text{const}$. The principal stress state of the shell is described by the membrane solution for a continuous shell:

$$T_r^0 = p_0 h, \quad T_\theta^0 = p_0 h, \quad S_{r\theta}^0 = 0, \tag{1}$$

where $p_0 h = pR/2$, R is the radius of the midsurface of the shell; h is its thickness.

The perturbation of the stress state caused by the inclusions can be found from the homogeneous system of governing differential equations of thin transversely isotropic shells proposed in [3, 5] and based on the refined Timoshenko-type theory that accounts for the transverse-shear strains. Let us represent them as

$$\nabla^2\nabla^2 U - \nabla^2 w = 0,$$

$$\nabla^2\nabla^2 w + \nabla^2 U - 2\delta\nabla^2\nabla^2 U = 0,$$

$$(1-\nu)\delta\nabla^2\chi - \chi = 0, \tag{2}$$

[1]V. I. Vernadskii National University of Tavriya, 4 Yaltenskaya St., Simferopol, Ukraine 95007; e-mail: chekhov40@mail.ru. [2]Donetsk National University, 24 Universitetskaya St., Donetsk, Ukraine 83055; e-mail: zakor@matfak.dongu.donetsk.ua. Translated from Prikladnaya Mekhanika, Vol. 47, No. 4, pp. 111–118, July 2011. Original article submitted April 6, 2010.

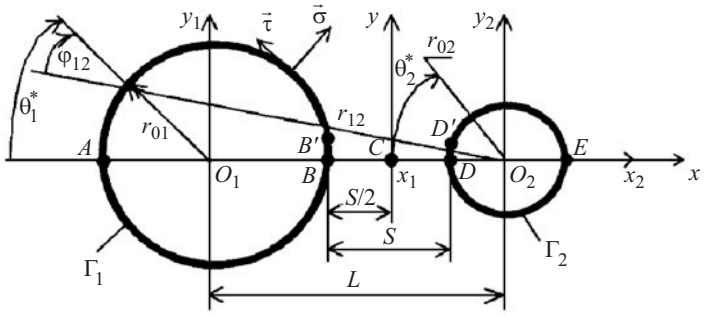

Fig. 1

where U, w, and χ are the unknown stress, deflection, and transverse-shear functions; $\nabla^2 = \frac{\partial^2}{\partial\rho^2} + \frac{1}{\rho}\frac{\partial}{\partial\rho} + \frac{1}{\rho^2}\frac{\partial^2}{\partial\theta^2}$ is the Laplacian in the polar coordinate system (ρ, θ), where $\rho = r/\sqrt{cR}$ is the dimensionless relative position vector; $r \cdot e^{i\theta} = x + iy$, $\delta = (Ehc)/(2KR)$ is the dimensionless relative compliance (to transverse shear) parameter, where $K = \mu G_1 h$, $c = h/\sqrt{12(1-\nu^2)}$, E is Young's modulus; ν is Poisson's ratio; G_1 is the transverse shear modulus; $\mu = 5/6$ is the shear coefficient.

The following five boundary conditions for strains are specified on each boundary Γ_q of the rigid inclusion:

$$\varepsilon_{\tau\tau}\big|_{\Gamma_q} = 0, \quad \kappa_{\tau\tau}\big|_{\Gamma_q} = 0, \quad \kappa_{\tau\nu}\big|_{\Gamma_q} = 0, \quad \kappa_{n\tau}\big|_{\Gamma_q} = 0, \quad Q_\tau\big|_{\Gamma_q} = 0, \tag{3}$$

where $q = \overline{1,2}$ is the number of hole boundary on which boundary conditions are prescribed.

The boundary strains (3) are expressed as

$$Eh\varepsilon_{\tau\tau} = (T_\tau + T_\tau^0) - \nu(T_\sigma + T_\sigma^0),$$

$$\frac{Eh^2}{2}\kappa_{\tau\tau} = \frac{6}{h}(G_\tau - \nu G_\sigma) - \frac{\delta\sqrt{3-3\nu^2}}{\rho}\sqrt{\frac{R}{c}}Q_\sigma,$$

$$\frac{Eh^2}{2}\kappa_{\tau\nu} = \frac{6(1+\nu)}{h}H_{\sigma\tau} - \delta\sqrt{3-3\nu^2}\sqrt{\frac{R}{c}}\frac{dQ_\tau}{d\sigma},$$

$$Ehc^2\kappa_{n\tau} = \frac{dT}{d\sigma} - (1+\nu)\frac{dS_{\sigma\tau}}{d\tau} - \delta\sqrt{\frac{R}{c}}Q_\sigma. \tag{4}$$

2. Problem-Solving Method. The solutions of the homogeneous system of differential equations (2) decreasing in absolute magnitude with distance from Γ_q, according to [3, 5], have three different analytic forms, depending on the range of variation in the parameter δ. The functions U and w are defined to have cylindrical and polyharmonic (power) components: $U = U_c + U_p$, $w = w_c + w_p$. If the boundaries are symmetric about the x-axis for $\delta > 1$, the solutions have the form

$$U_c(\rho_q, \theta_q) = \sum_{q=1}^{2}\sum_{n=0}^{\infty}\left[A_{qn}K_n(\alpha\rho_{qk}) + B_{qn}K_n(\beta\rho_{qk})\right]\cos n\theta_{qk}, \tag{5}$$

$$U_p(\rho_q, \theta_q) = \sum_{q=1}^{2}\sum_{n=1}^{\infty}D_{qn}\frac{1}{\rho_{qk}^n}\cos n\theta_{qk}, \tag{6}$$

$$w_c(\rho_q, \theta_q) = \sum_{q=1}^{2}\sum_{n=0}^{\infty}\left[\alpha^2 A_{qn}K_n(\alpha\rho_{qk}) + \beta^2 B_{qn}K_n(\beta\rho_{qk})\right]\cos n\theta_{qk}, \tag{7}$$

$$w_{\mathrm{p}}(\rho_q,\theta_q)=\sum_{q=1}^{2}\sum_{n=1}^{\infty}C_{qn}\,\frac{1}{\rho_{qk}^{n}}\cos n\theta_{qk}, \tag{8}$$

$$\chi(\rho_q,\theta_q)=\sum_{q=1}^{2}\sum_{n=1}^{\infty}M_{qn}K_n(\lambda\rho_{qk})\sin n\theta_{qk}, \tag{9}$$

where $A_{q,n}, B_{q,n}, C_{q,n}, D_{q,n}, M_{q,n}$ are unknown real constants; I_m and K_m are the modified Bessel functions of the first and second kinds (K_m are also called Macdonald functions); $\alpha=\sqrt{\delta+\sqrt{\delta^2-1}}, \beta=1/\alpha, \lambda=1/\sqrt{(1-\nu)\delta}, \rho_{qk}=r_{qk}/\sqrt{cR}$; where r_{qk} is the position vector coming from the center O_k of the boundary Γ_k to the boundary Γ_q (Fig. 1); θ_{qk} is the angle between the Ox-axis and the position vector r_{qk} ($k=\overline{1,2}$).

To separate variables in the unknown functions in the qth coordinate system, we will follow Guz who proposed in [3, 6] to use Graf's theorem for cylindrical functions in (5), (7), (9) and to expand each term of the power part of solution (6), (8) into the Laurent series. Doing so give the expressions

$$U_{\mathrm{c}}(\rho_q,\theta_q)=\sum_{q=1}^{2}\sum_{n=0}^{\infty}\Bigg\{A_{qn}K_n(\alpha\rho_{0q})+I_n(\alpha\rho_{0q})e_n\sum_{p=0}^{\infty}e_{np}A_{3-q\,p}(-1)^p\Big[K_{n-p}(\alpha l)+K_{n+p}(\alpha l)\Big]$$

$$+B_{qn}K_n(\beta\rho_{0q})+I_n(\beta\rho_{0q})e_n\sum_{p=0}^{\infty}e_{np}B_{3-q\,p}(-1)^p\Big[K_{n-p}(\beta l)+K_{n+p}(\beta l)\Big]\Bigg\}\cos n\theta_q, \tag{10}$$

$$U_{\mathrm{p}}(\rho_q,\theta_q)=\sum_{q=1}^{2}\left[\sum_{n=0}^{\infty}\sum_{p=1}^{\infty}\frac{e_{np}(-1)^p(p+n-1)!\rho_{0q}^{n}\cos n\theta_q}{(p-1)!n!l^{p+n}}D_{3-q\,p}+\sum_{n=1}^{\infty}D_{qn}\frac{\cos n\theta_q}{\rho_{0q}^{n}}\right], \tag{11}$$

$$\chi(\rho_q,\theta_q)=\sum_{q=1}^{2}\sum_{n=1}^{\infty}\Bigg\{I_n(\lambda\rho_{0q})e_n\sum_{p=0}^{\infty}e_{np}M_{3-q\,p}(-1)^p\Big[K_{n-p}(\lambda l)+K_{n+p}(\lambda l)\Big]+M_{qn}K_n(\lambda\rho_{0q})\Bigg\}\sin n\theta_q, \tag{12}$$

where $l=L/r_{01}$ is the dimensionless relative distance between the centers of the inclusions (Fig. 1); if $k=q$, then $\theta_{qk}=\theta_q$, $\rho_{qk}=\rho_{0q}$, i.e., dimensionless radii of the inclusions; $e_n=\begin{cases}1/2, & n=0,\\ 1, & n\neq 0,\end{cases}$ $e_{np}=\begin{cases}1, & q=1,\\ (-1)^{n+p}, & q=2\end{cases}$; w_{c} and w_{p} can be transformed in a similar way.

The expressions for the forces and moments corresponding to the homogeneous solutions (5)–(12) are the following:

$$T_\theta=\frac{\partial^2 U}{\partial\rho^2},\quad T_r=\nabla^2 U-T_\theta,\quad H_{r\theta}=(1-\nu)c\left[\delta\left(\nabla^2\chi-2\frac{\partial^2\chi}{\partial\rho^2}\right)-\frac{\partial}{\partial\rho}\left(\frac{1}{\rho}\frac{\partial g}{\partial\theta}\right)\right],$$

$$G_r=c\left[\frac{2}{\lambda^2}\frac{\partial}{\partial\rho}\left(\frac{1}{\rho}\frac{\partial\chi}{\partial\theta}\right)-\frac{\partial^2 g}{\partial\rho^2}-\nu\left(\frac{1}{\rho}\frac{\partial g}{\partial\rho}+\frac{1}{\rho^2}\frac{\partial^2 g}{\partial\theta^2}\right)\right],\quad G_\theta=-(1+\nu)c\nabla^2 g-G_r,$$

$$Q_r=\sqrt{\frac{c}{R}}\frac{\partial}{\partial\rho}\left(\frac{1}{\rho}\frac{\partial\chi}{\partial\theta}-\frac{\partial}{\partial\rho}\nabla^2 g\right),\quad Q_\theta=-\sqrt{\frac{c}{R}}\left(\frac{\partial\chi}{\partial\rho}+\frac{1}{\rho}\frac{\partial}{\partial\theta}\nabla^2 g\right),\quad S_{r\theta}=-\frac{\partial}{\partial\rho}\left(\frac{1}{\rho}\frac{\partial U}{\partial\theta}\right)$$

$$(g=w+2\delta\nabla^2 w-4\delta^2\nabla^2 U). \tag{13}$$

Substituting the forces and moments (13) with (9)–(12) into the boundary conditions (3) and equating the coefficient of like harmonics, we obtain an infinite system of linear algebraic equations for $A_{q,n}, B_{q,n}, C_{q,n}, D_{q,n}, M_{q,n}$. According to [3], this system should be supplemented with the following conditions for complex displacements: $C_{q,1}=0, D_{q,1}=0$. Moreover, in the

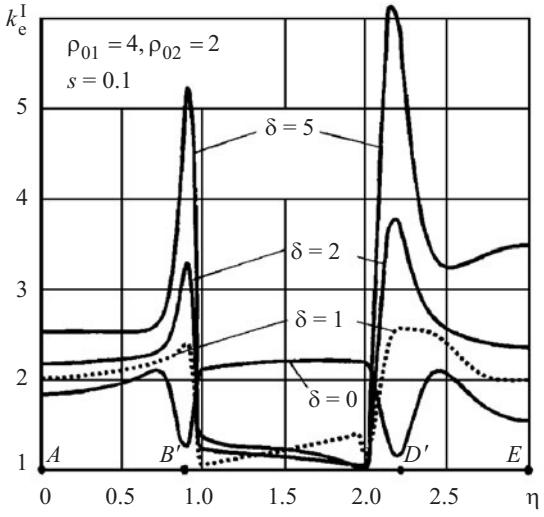

Fig. 2

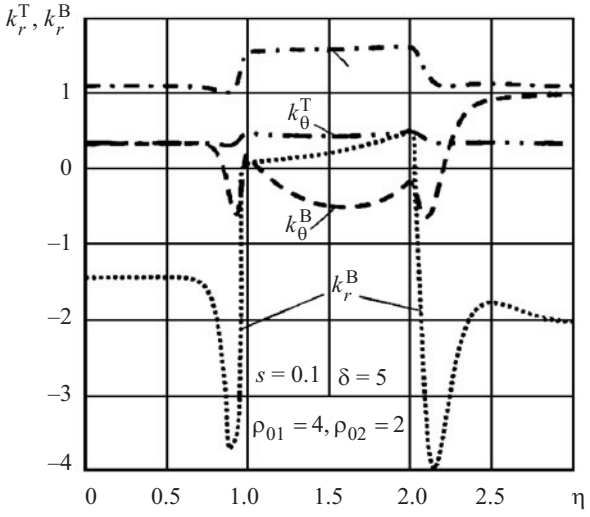

Fig. 3

0th and 1st harmonics, we omit the equations $\kappa_{\tau\nu}\big|_{\Gamma_q} = 0$, $\kappa_{n\tau}\big|_{\Gamma_q} = 0$, and $Q_\tau\big|_{\Gamma_q} = 0$ that are dependent, according to the identities in [1]. The resulting system is solved with the reduction method.

Substituting $A_{q,n}, B_{q,n}, C_{q,n}, D_{q,n}, M_{q,n}$ found by solving the system into formulas (5)–(9), we find the functions U, w, and χ. Next, we use formulas (13) and the membrane solution (1) to determine the forces and moments at given points, which will depend on the angles $\vec{\sigma}$, $\vec{\tau}$ (Fig. 1) upon passage to the directions φ_q using well-known transformation formulas [1].

3. Numerical Results. We numerically analyzed a transtropic spherical shell with two unequal circular rigid inclusions for different widths of the bridge between them and different values of δ. Poisson's ratio of the shell material $\nu = 0.3$. The shell is subject to internal pressure. The concentration factors for the membrane and bending stresses were calculated using the formulas

$$k_\theta^T = (T_\theta + T_\theta^0)/\, p_0 h, \qquad k_r^T = (T_r + T_r^0)/\, p_0 h,$$

$$k_\theta^B = 6G_\theta / \, p_0 h^2, \qquad k_r^B = 6G_r / \, p_0 h^2,$$

$$\tau_{r\theta}^T = (S_{r\theta} + S_{r\theta}^0)/\, p_0 h, \qquad \tau_{r\theta}^B = 6H_{r\theta} / \, p_0 h^2. \tag{14}$$

They were used to calculate the relative equivalent stresses using the energy theory of strength [3]:

$$k_\theta = k_\theta^T \pm k_\theta^B, \qquad k_r = k_r^T \pm k_r^B,$$

$$k_{r\theta} = \tau_{r\theta}^T \pm \tau_{r\theta}^B, \qquad k_e = \sqrt{k_r^2 + k_\theta^2 - k_r k_\theta + 3k_{r\theta}^2}. \tag{15}$$

Note that the signs "+" and "–" in formulas (15) correspond to the relative equivalent stresses on the outside and inside surfaces of the shell, k_e^O and k_e^I.

Figures 2–5 and Tables 1, 2 present the results for a shell with two rigid inclusions soldered in holes of radii $\rho_{01} = 4$ and $\rho_{02} = 2$. Here $\rho_{0q} = r_{0q} / \sqrt{cR}$ are the radii of the inclusions; $s = S / r_{01}$ is the width of the bridge between the inclusions.

The ordinate axis indicates k_e^I in Fig. 2, k_e^O in Fig. 4, and k_r^T, k_θ^T and k_r^B, k_θ^B in Figs. 3 and 5. The parameter η laid off along the abscissa axis (Figs. 2–5) takes the following values:

(i) $\eta = 2(q-1) + \theta_q^* / \pi$ for $2(q-1) \le \eta \le 2q-1$ describes half the boundary Γ_q of the inclusion, i.e., if there is symmetry about the *Ox*-axis, we have $0 \le \theta_q^* \le \pi$, where $\theta_q^* = \pi - \theta$ (Fig. 1);

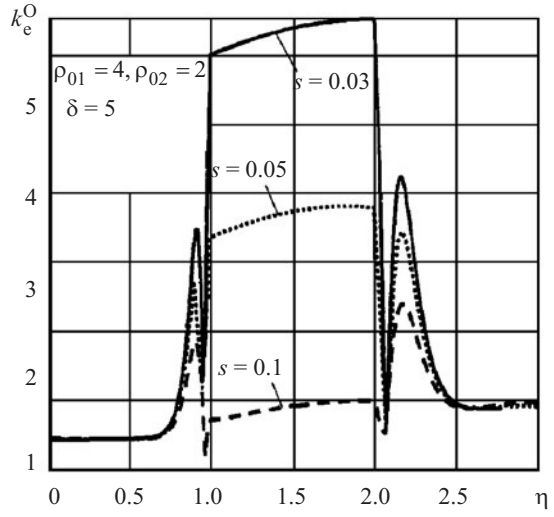

Fig. 4

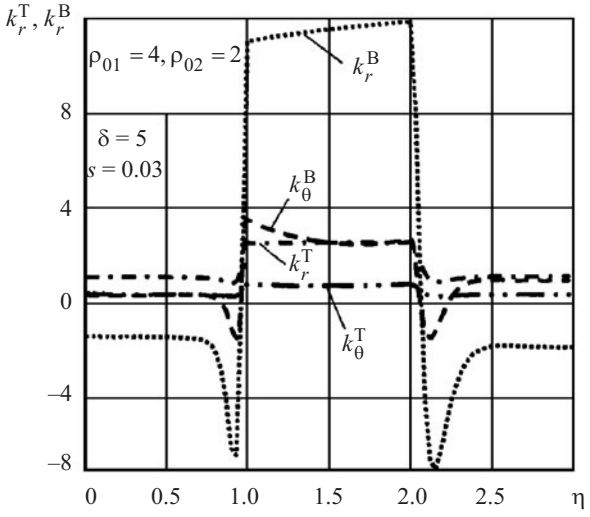

Fig. 5

(ii) $\eta = 1 + \dfrac{x_1 - r_{01}}{S}$ for $1 \le \eta \le 2$ describes the bridge s, i.e., when $r_{01} \le x_1 \le r_{01} + S$.

Figure 2 shows the distribution of the stress k_e^I for $s = 0.1$ depending on the parameter δ (its values are indicated near the curves). When $\delta = 0$, use is made of the classical theory of shallow isotropic shells based on the Kirchhoff–Love hypothesis [3]. It can be seen that the relative equivalent stresses k_e^I near the bridge increases with the parameter δ. For example, as the parameter δ increases from 1 to 5, the maximum stress k_e^I at the point D' increases by a factor of 2.4. Figure 3 shows that the bending stress k_r^B contributes the most.

The dependence of the stress state of the shell on the width of the bridge s is demonstrated by Figs. 4 and 5 for $\delta = 5$ and by Tables 1 and 2 for $\delta = 5, 1, 0$. The value of s is indicated near each curve in Fig. 4. It can be seen that the less the bridge width s, the higher the maximum stresses k_e near and on the bridge. Comparing cases (a) of Tables 1 and 2, we see that as the bridge width s decreases from 0.5 to 0.06, the maximum relative equivalent stresses k_e^I and k_e^O at the point D' increase by factors 2 and 3.4, respectively (underlined values in the tables).

The narrower the bridge, the stronger the effect of the compliance parameter. For example, for $s = 0.5$, $\delta = 5$ in Table 1, the maximum stress k_e at the dangerous point D' in case (a) is greater by 66% than in case (b) and by 88% than in case (c). For $s = 0.06$ in Table 2, this stress at the points D and D' in case (a) is higher by 107% than in case (b) and by 153% than in case (c). As follows from Tables 1, 2 and Figs. 3, 5, this is mainly due to the increase in the bending stress k_r^B.

4. Reliability of the Results. We tested the accuracy of satisfying the boundary conditions through the direct calculation of the forces and moments on the boundaries using series (5)–(9), i.e., not using Graf's theorem and Laurent series. To this end, we used Maple 10 software. The accuracy of computation can be varied by assigning a value to the system variable Digits and setting the number n of harmonics in (5)–(9). For example, if $n = 50$ and Digits = 77, the error of satisfying the boundary conditions does not exceed 0.004% of the maximum stress (i.e., 1.0) in the solid shell in case (a) of Table 1 and 0.1% in case (a) of Table 2.

For comparison to a spherical shell with one rigid inclusion [10], we calculated the case where the rigid inclusions do not interact, i.e., $s = 20$. The obtained results are in good agreement with those in [10].

We also tested the accuracy of satisfying the differential equations (2) by the functions U, w, χ with coefficients determined after the solution of the system. The absolute error does not exceed 10^{-72} for Digits = 77.

Conclusions. We have found the analytic solution for the stress state of a transversely isotropic shallow spherical shell with two circular perfectly rigid inclusions using the refined Timoshenko-type theory that accounts for the transverse-shear strains. The cases of closely spaced rigid inclusions of different radii in a shell under internal pressure have been numerically

TABLE 1

Case	k_e, k_r, k_θ	$\rho_{01} = 4$		$s = 0.5$	$\rho_{02} = 2$		
		A	*B*	*C*	*D*	*D′*	*E*
(a) $\delta = 5$	k_e	$\theta_1^* = 0$	$\theta_1^* = \pi$	$s/2$	$\theta_2^* = 0$	$\theta_2^* = 7\pi/65$	$\theta_2^* = \pi$
	k_r^T	1.084	1.121	1.075	1.221	1.206	1.118
	k_θ^T	0.325	0.336	0.821	0.366	0.362	0.335
	k_r^B	–1.448	–2.203	–1.995	–2.422	–2.269	–1.876
	k_θ^B	0.314	–0.029	0.245	0.199	0.311	0.908
	k_e^O	0.880	1.264	1.723	1.563	1.842	1.750
	k_e^I	2.526	3.157	2.826	3.563	3.609	3.317
(b) $\delta = 1$	k_e	$\theta_1^* = 0$	$\theta_1^* = \pi$	$s/2$	$\theta_2^* = 0$	$\theta_2^* = \pi/3$	$\theta_2^* = \pi$
	k_r^T	1.146	1.174	1.106	1.289	1.216	1.217
	k_θ^T	0.344	0.352	0.633	0.387	0.365	0.365
	k_r^B	–1.105	–1.034	–0.563	–0.883	–1.073	–1.037
	k_θ^B	–0.096	–0.118	–0.064	0.080	0.120	0.037
	k_e^O	0.230	0.204	0.556	0.439	0.433	0.349
	k_e^I	2.066	2.015	1.452	2.036	2.179	2.109
(c) $\delta = 0$	k_e	$\theta_1^* = 0$	$\theta_1^* = \pi$	$s/2$	$\theta_2^* = 0$	$\theta_2^* = 3\pi/8$	$\theta_2^* = \pi$
	k_e^O	0.229	0.664	1.118	1.202	0.311	0.639
	k_e^I	1.895	1.563	0.951	1.200	1.918	1.712

TABLE 2

Case	k_e, k_r, k_θ	$\rho_{01} = 4$			$s = 0.06$	$\rho_{02} = 2$		
		A	*B′*	*B*	*C*	*D*	*D′*	*E*
(a) $\delta = 5$	k_e	$\theta_1^* = 0$	$\theta_1^* = 11\pi/12$	$\theta_1^* = \pi$	$s/2$	$\theta_2^* = 0$	$\theta_2^* = 8\pi/49$	$\theta_2^* = \pi$
	k_r^T	1.085	0.941	1.871	1.912	1.935	1.021	1.099
	k_θ^T	0.325	0.282	0.561	4.234	0.580	0.306	0.330
	k_r^B	–1.442	–4.964	3.878	0.492	4.479	–5.169	–1.972
	k_θ^B	0.314	–0.888	1.250	0.292	0.706	–0.682	0.957
	k_e^O	0.875	4.961	5.091	5.794	5.877	6.252	1.882
	k_e^I	2.522	6.483	1.767	2.428	2.483	7.536	3.428
(b) $\delta = 1$	k_e	$\theta_1^* = 0$	$\theta_1^* = 9\pi/10$	$\theta_1^* = \pi$	$s/2$	$\theta_2^* = 0$	$\theta_2^* = \pi/5$	$\theta_2^* = \pi$
	k_r^T	1.168	0.880	2.293	2.340	2.418	0.949	1.193
	k_θ^T	0.350	0.264	0.688	0.528	0.725	0.285	0.358
	k_r^B	–1.023	–1.603	1.757	1.597	1.742	–1.734	–0.962
	k_θ^B	–0.087	–0.334	0.380	0.288	0.811	0.111	–0.142
	k_e^O	0.229	1.203	3.635	3.600	3.643	2.756	0.224
	k_e^I	2.008	2.686	0.465	0.657	0.723	1.318	1.954
(c) $\delta = 0$	k_e	$\theta_1^* = 0$	$\theta_1^* = 17\pi/24$	$\theta_1^* = \pi$	$s/2$	$\theta_2^* = 0$	$\theta_2^* = \pi/2$	$\theta_2^* = \pi$
	k_e^O	0.342	0.219	1.856	1.772	1.581	0.133	0.919
	k_e^I	1.827	2.141	2.655	2.843	2.979	2.111	1.531

analyzed. The stresses in the shell increase considerably with decrease in the width of the bridge between the rigid inclusions and with increase in the transverse-shear parameter.

REFERENCES

1. A. N. Guz, I. S. Chernyshenko, Val. N. Chekhov, Vik. N. Chekhov, and K. I. Shnerenko, *Cylindrical Shells Weakened by Holes* [in Russian], Naukova Dumka, Kyiv (1974).
2. A. N. Guz, I. S. Chernyshenko, Val. N. Chekhov, Vik. N. Chekhov, and K. I. Shnerenko, *Theory of Thin Shells Weakened by Holes*, Vol. 1 of the five-volume series *Methods of Shell Design* [in Russian], Naukova Dumka, Kyiv (1980).
3. A. N. Guz, I. S. Chernyshenko, and K. I. Shnerenko, *Spherical Bottoms Weakened by Holes* [in Russian], Naukova Dumka, Kyiv (1970).
4. V. N. Chekhov, "Stability of layered materials with zero in-plane strains," *Int. Appl. Mech*., **46**, No. 12, 1351–1361 (2010).
5. I. S. Chernyshenko, E. A. Storozhuk, and I. B. Rudenko, "Elastoplastic state of flexible spherical shells with a reinforced elliptic hole," *Int. Appl. Mech*., **44**, No. 12, 1397–1404 (2008).
6. A. N. Guz, E. A. Storozhuk, and I. S. Chernyshenko, "Nonlinear two-dimensional static problems for thin shells with reinforced curvilinear holes," *Int. Appl. Mech*., **45**, No. 12, 1269–1300 (2009).
7. O. A. Kondratenko, "Stress state around a circular hole in a prestressed transversely isotropic spherical shell," *Int. Appl. Mech*., **44**, No. 2, 167–173 (2008).
8. V. V. Panasyuk and M. P. Savruk, "On the problem of determination of stress concentration in a stretched plate with two holes," *J. Math. Sci*., **162**, No. 1, 132–148 (2009).
9. E. A. Tkachenko and V. N. Chekhov, "Stability of layered coatings under biaxial termomechanical loading," *Int. Appl. Mech*., **45**, No. 12, 1349–1356 (2009).
10. S. V. Zakora and Val. N. Chekhov, "Stress state of a transversely isotropic spherical shell with a rigid circular inclusion," *Int. Appl. Mech*., **41**, No. 12, 1384–1390 (2005).